



Design and realization of a box type solar cooker with thermal storage dedicated to the rural regions of the oriental district

S.Talbi, K. Kassmi*, A. Lamkaddem, R. Malek

Laboratoire Électromagnétisme, Traitement de Signal & Énergies Renouvelables LETSER,
Mohamed Premier University, Faculty of Sciences, Department of Physics, Oujda 60000, Morocco

Received 22 Jun 2016,

Revised 15 Dec 2017,

Accepted 17 Dec 2017

Keywords

- ✓ Solar oven box-type,
- ✓ Reflectors,
- ✓ Thermal Storage,
- ✓ Thermal resistance,
- ✓ Thermal power,
- ✓ Thermal efficiency,
- ✓ Temperature,

khkassmi@yahoo.fr,
Phone: (+212) 678075214

Abstract

In this article, the work presented concerns the design and the simulation of the operation and the experimentation of a solar cooker, of the box type with three reflectors. In order to improve the efficiency of the cooker, we integrated the heat storage of the temperature with the salt placed at the base of the cooker. The first obtained results show a thermal resistance of the cooker of the order 0.51K.W^{-1} , under ansolar radiation of 1000W/m^2 , temperatures, powers and efficiencies respectively reach 140°C , 225.49W and 93% . Regarding the temperature storage, we showed that after one hour without solar radiation, the storage ensures the maintenance of the temperature of the order 40% of the value with illumination. The comparison between the experimental results and those simulated shows a good agreement and consequently the validation of the operation and the insulation of the cooker proposed during this work.

1. Introduction

Deforestation in the world by the inhabitants and the emissions of certain polluting gases linked to fossil fuels (oil, etc.) have intensified the natural phenomenon of the greenhouse effect and lead to the warming of the temperature on earth [1, 2]. This phenomenon is likely to have important consequences for the climate and ecosystems of the planet. The international community has therefore mobilized to propose alternatives to limit the use of forest woods and limit the concentrations of greenhouse gases in the atmosphere, with the aim of halving emissions worldwide before 2050 [3].

In this context, our goal, in collaboration with the socio-economic sectors of the Eastern region of Morocco (Man and Environment Association of Berkane AHEB, Province of Berkane, company EVES Energies, ...), is the promotion and development of cookers solar and photovoltaic kits in the kitchens and homes of the inhabitants, especially those who daily exploit the forests of the region. We offer high-performance equipment based on renewable energies and adaptable to their lifestyles (cooking, lighting ..). This equipment improves their living conditions and contains no moving parts; it requires little maintenance and it is silent. It produces no pollutants and preserves the forests and the environment of the Oriental region.

In the literature, several solar cookers are proposed [4,5]: parabolic cooker with high cooking temperatures between 200°C and 300°C [6], cookers with reflective panels, consisting of different reflective flat panels and a black container encased in a plastic bag. This equipment has many disadvantages such as high cost, large size, risk of food burns, longer cooking time and uncontrollable temperature. These types of cookers whose mode of operation is considered complicated and random do not interest users in their daily cooking mode.

Currently, the designers of solar cookers are moving towards the box cookers, since they have a lot of advantages such as simple to carry out, easy operation, very stable, less expensive, and no risk of burns. Cookers are already presented in the literature [7-16], but there is usually a lack of in-depth analyses (simulations and experiments), and limitations of performance (Temperature not exceeding 120°C - 130°C) without taking into account of temperature storage. This is necessary to stabilize the temperature following possible variations in solar radiation.

In this context, we are conducting research on improving the performance of box-type cookers in order to achieve user-controllable cooking temperatures of 250 °C - 300 °C and taking into account thermal storage by the user (sand or salt). This is achieved by combining solar thermal energy directly from the sun and electrical energy that heats thermal resistance by photovoltaic panels [17-20].

In this paper, we present the first results concerning the design and in-depth analysis of the thermal operation of the box-type cooker using only solar thermal energy. After describing the structure and operation of the cooker prototype, we present the models of the heat transfer in the different blocks of the cooker, the equivalent resistance, the power and the thermal efficiency of the cooker. In our study, special attention will be paid to the storage of temperature using mineral salts, since they are known by their storage capacities and insulation of the interior of the cooker. Then, we present the results of the numerical simulations and the experimental validation by experimenting the functioning of the cooker conceived during sunny days and presenting variations of the intensity of the solar radiation.

2. Structure and models of heat transfer.

2.1. Structure and operation of the solar cooker

Figure 1 shows the diagram of the box type solar cooker, which is the subject of our study. The different blocks of this cooker are:

- Three external reflectors whose role is to capture the maximum solar radiation and the reflection towards the interior of the cooker. In Figure 1, we have shown only one of the clarity and readability of the cooker.
- Four interior reflectors (Cooker sides) whose role is to reflect solar radiation on the absorber,
- Double glazing (Windows 1 and 2) which, for the purpose of keeping the heat inside the greenhouse,
- An absorber whose role is to transform solar radiation into heat. It behaves like a black body thanks to a coating by black paint at high temperature,
- A thermally insulated box (wood, corks, stainless steel) to minimise heat loss in the solar cooker,
- Thermal storage medium, filled with mineral salts (NaCl).

The principle of operation, or heating, thermal of the solar cooker, is as follows:

- Through Direct Transmission (A), solar energy is transmitted directly into the cooker,
- The reflectors reflect solar radiation to the window 1 (B). Then, on the window 1, the radiation is reflected and transmitted to the window 2 (C). These results in the heating of the two windows and in particular the space between them.
- The window 2 reflected and transmitted the solar radiation (D) to the absorber (E). The latter absorbs the solar radiation and the temperature of the container rises gradually.
- Reflections by the internal reflectors (F) to the absorber (E). This helps in heating the interior of the cooker.
- Through the phenomenon of the greenhouse effect, solar radiation is trapped inside the cooker (G). As a result, heat is stored inside the cooker and the internal temperature increases with the intensity of the radiation.
- Storage of the temperature by exploiting the latent heat of some materials (mineral salts (NaCl), sand, ...). The temperature is stored in these materials for a period longer than 1 hour in order to stabilize the temperature as a result of any variations in the intensity of the radiation.

In our study, we analyse the operation of the cooker by modelling the temperatures of nodes 1 to 6 shown in Figure 1: Glass 1 (Tv1), Glass 2 (Tv2), Container lid (Tcr), Water (Tf), Container (Tr), Thermal storage (Tst).

2.2. Models of Thermal Transfer in box type solar cooker

In this section, we establish the basic notions governing transient thermal transfer [21], the equations adapted to our prototype (Figure 1). This allows us to analyse in depth the operation of the box-type solar cooker in order to improve its thermal performance (Temperature at each node, resistance, power and efficiency) and validate the experimental results. In our study, we consider:

- ✓ 6 nodes of the cooker of the structure (Figure 1): first window, second window, container lid, containers, water in the container and storage materials.
- ✓ hypotheses:
 - Heat exchanges are unidirectional,
 - The temperature is uniform in each knot of the cooker,
 - The wind speed is constant,

- The thermo-physical properties of the glass, the air and the absorber are considered constant within the operating temperature margin of the cooker,
- The heat exchange coefficients are constant to facilitate the numerical solution of equations, and to avoid the computation complexity of nonlinear system [25],
- The variation of the internal energy at each node is equal to the sum of the quantities of heat exchanged by the radiation and convection heat transfer modes [21-25].

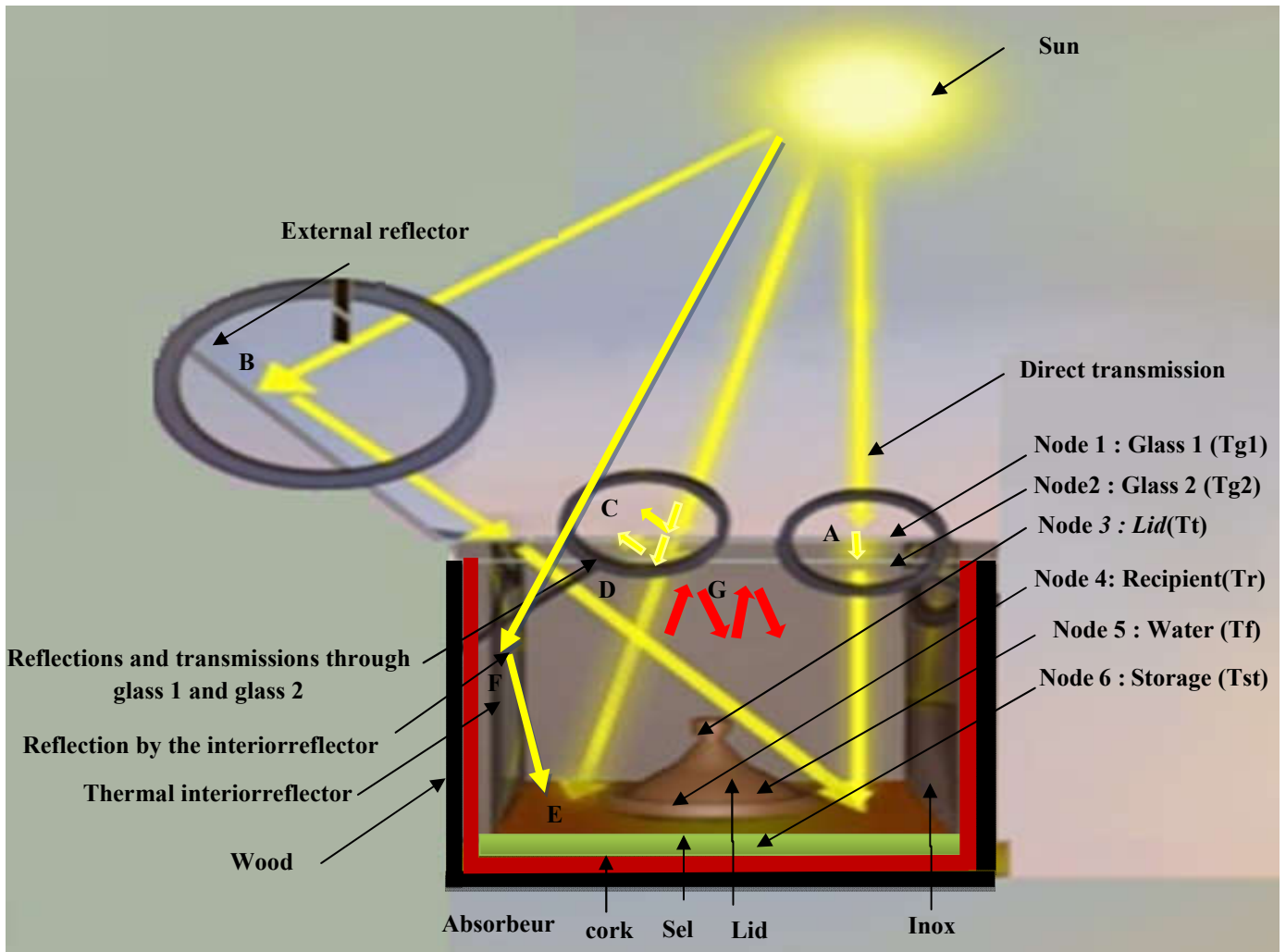


Figure 1: Structure of the box-type solar cooker, transmissions and reflections (or absorption) of the radiation (A to G), nodes used and their respective temperatures.

- A: Direct transmission,
- B: Reflections by reflectors,
- C: Reflections and transmissions through the glass 1,
- D: Reflections and transmissions through the glass 2,
- E: Absorption by the Absorber,
- F: Absorption by the Absorber,
- G: Greenhouse effect inside the box.

For a clearly or heat flux and an ambient temperature (T_{amb}), at each node, the models of the heat exchange are written as follows [21-25]:

✓ **Node 1 :**

At this node, the heat exchange model of the first temperature window T_{g1} is written as a function of the temperatures of the two windows (T_{g1} , T_{g2}), ambient temperature T_{amb} , temperature of the sky T_c , radiating heat flux (Q_1 , Q_2 , Q_4) and convective heat (Q_3 , Q_5) [22-25]:

$$\begin{aligned}
(mcp)_{v1} \frac{dT_{v1}}{dt} &= Q1 + Q2 - Q3 - Q4 + Q5 \\
&= \alpha_g A_v [G + G \rho \cos(90 - \alpha)] \\
&+ A_g \sigma \varepsilon_g (T_{g2}^4 - T_{g1}^4) \\
&- h_{g,g1-int1} \cdot A_v \cdot (T_{g2} - T_{g1}) \\
&+ h_{g-amb} A (T_{v1} - T_{amb})
\end{aligned} \tag{1}$$

Where,

$(mcp)_{v1}$: mass heat of the first constant pressure pane,

T_c : temperature of the sky, given by [26] :

$$T_c = 0.0552 \cdot T_{amb}^{1.5}$$

$Q1$: solar radiation heat flux absorbed by glass 1. It is a function of the glass absorptivity (α_g), glass surface (A_v), solar radiation (G) and the angle of the outer reflector (α),

$Q2$: heat flux exchanged by radiation between the glass 2 and the glass 1. It is a function of the temperatures of the two panes (T_{g1} , T_{g2}), the glass emissivity ε_g , Boltzmann constant σ , area of glass A_g ,

$Q3$: convective heat flux exchanged between the window 1 and the interior 1 (between the window 1 and the window 2). It is a function of the temperatures of the two panes (T_{g1} , T_{g2}), glass surface A_v , convective exchange coefficient $h_{g1-int1}$,

$Q4$: radiant heat flux exchanged between the glass1 and the sky. It is a function of the temperatures of the two panes (T_{g1} , T_{amb}), the glass emissivity ε_g , the Boltzmann constant σ , and the glass surface A_g ,

$Q5$: heat flow exchanged by convection between the window 1 and the ambient. It is a function of the temperatures of the two panes (T_{g1} , T_{amb}), convective heat exchange coefficient h_{g-amb} , glass surface A_g .

✓ **Node 2 :**

At this node, the heat exchange model of the second temperature window T_{v2} is written as a function of the temperatures of the two panes (T_{v1} , T_{v2}), ambient temperature T_{amb} , temperature of the container lid T_{cr} , internal temperature T_{int2} , flow of radiating heat (Q_6 , Q_7 , Q_{11}), and convective heat flux (Q_8 , Q_{10}) [22-25]:

$$\begin{aligned}
(mcp)_{g2} \frac{dT_{g2}}{dt} &= Q6 - Q7 - Q8 + Q9 + Q_{10} + Q_{11} \\
&= \alpha_g \cdot \tau_g \cdot A_g \cdot [G + G \rho \cos(90 - \alpha)] \\
&- A_g \sigma \varepsilon_g (T_{g2}^4 - T_{g1}^4) - h_{g2,int2} \cdot A \cdot (T_{g2} - T_{g1}) \\
&+ A_{cr} \sigma \varepsilon_{cr} (T_{cr}^4 - T_{v2}^4) + h_{v,int2} \cdot A \cdot (T_{int2} - T_{v2}) \\
&+ A_v \sigma \varepsilon_r (T_r^4 - T_{v2}^4)
\end{aligned} \tag{2}$$

Where,

$(mcp)_{g2}$: Mass heat of the second window at constant pressure,

T_{int2} : Interior temperature between glass 2 and the indoor environment. It is a function of the window temperature 1 (T_{v1}), the container lid (T_{cr}), and the container (T_r):

$$T_{int2} = \frac{T_{v1} + T_r + T_{cr}}{3}$$

$Q6$: Solar power absorbed by the outer pane. It is a function of the glass transitivity (τ_g), the glass surface (A_v), the solar radiation (G) and the angle of the outer reflector (α),

- Q7: heat flux exchanged by radiation between the glass 2 and the glass 1. It is a function of the temperatures of the two panes (T_{g1} , T_{g2}), the glass emissivity ε_v , the Boltzmann constant σ and the glass surface A_g ,
- Q8: heat flux exchanged between the glass 2 and the inside 2. It is a function of the temperatures of the two panes (T_{g1} , T_{g2}), the glass surface A_v , and the convective exchange coefficient $h_{g2,int2}$,
- Q9: heatflux exchanged by radiation between the container lid and the window 2. It is a function of the temperatures of the glass pane 2 and the container lid (T_t , T_{g2}), the surface of the container lid A_t , the emissivity of the container lid ε_t and constant of Boltzmann σ ,
- Q10: heat flux exchanged by convection between the interior 2 and the glass 2. It is a function of the temperatures of the interior and the window 2 (T_{int2} , T_{g2}), glass surface A_g and convective exchange coefficient $h_{g2,int2}$.
- Q11: heat flux exchanged by convection between the interior 2 and the glass 2. It is a function of the temperatures of the interior and the window 2 (T_{int2} , T_{g2}), glass surface A_v and convective exchange coefficient g

✓ **Node 3 :**

At this node, the heat exchange model on the temperature container lid T_t is written as a function of the temperatures of the container lid and the glass pane 2 (T_t , T_{g2}), the container lid temperatures and the interior temperature. (T_t , T_{int2}), lid, container and water temperatures (T_t , T_f), radiating heat fluxes (Q12, Q14, Q15, and Q16) and convective heat fluxes (Q13, Q14) [22-25]:

$$\begin{aligned}
 m_{cr} \cdot Cp_{cr} \frac{dT_{cr}}{dt} &= Q12 + Q13 + Q14Q15-Q16 \\
 &= A_{cr} \sigma \varepsilon_{cr} (T_t^4 - T_{v2}^4) + h_{t,int2} A_{cr} (T_t - T_{int2}) \\
 &\quad + A_t [G + G \rho \cos(90 - \alpha)] \tau_g^2 \alpha_t \\
 &\quad - h_{t,int3} A_t (T_t - T_f) - A_t \sigma \varepsilon_t (T_t^4 - T_f^4)
 \end{aligned} \tag{3}$$

Where,

$m_{cr} \cdot Cp_{cr}$: Mass heat of the constant pressure container lid,

- Q12: heat flux exchanged by radiation between the container lid and the window 2. It is a function of the temperatures of the window 2 and the container lid (T_t , T_{g2}), the container lid surface A_t , the emissivity of the container lid ε and constant of Boltzmann σ .
- Q13: heat flow exchanged by convection between the lid of the container and the interior 2. It is a function of the temperatures of the lid of the container and the inner 2 (T_t , T_{int2}), surface of the container lid A_t and convective exchange coefficient $h_{t, int2}$.
- Q14: solar power absorbed by the container lid. It is a function of the transmissivity of the glass (τ_g), the absorptivity of the container lid (α_t), the surface of the container lid A_t , solar radiation (G) and the external reflector angle (α).
- Q15: heat flux exchanged by convection between the interior 3 (between the container lid and the fluid surface) and the container lid. It is a function of the temperatures of the lid of the container and the water (T_t , T_f), surface of the lid of the container at and convective exchange coefficient h_{t-int3} .
- Q16: heat flux exchanging radiation between the container lid and the fluid. It is a function of the water container lid temperatures (T_t , T_f), container lid area at emissivity of container lid ε_t and Boltzmann constant σ .

✓ **Node 4 :**

At this node the model of heat exchange on the temperature container T_r is written as a function of the temperatures of the interior 2 and container (T_{int2} , T_t), container temperatures and water (T_r , T_f), radiating heat fluxes (Q18, Q19) and convective heat fluxes (Q17, Q20) [22-25] :

$$\begin{aligned}
m_r C_{p_r} \frac{dT_r}{dt} &= Q17 + Q18 - Q19 - Q20 \\
&= h_{r,int2} \cdot A(T_{int2} - T_r) + 4 * \\
&\quad \sum_{i=1}^n \rho \cdot S_{ref,n} [G + G \rho \cos(90 - \alpha)] \tau_g^2 \cdot \cos(90 - \theta_{ref,n}) \\
&\quad - A_r \sigma \epsilon_r (T_r^4 - T_f^4) - A_m h_{r,fl} (T_r - T_f)
\end{aligned} \tag{4}$$

Where,

$m_r C_{p_r}$: Mass heat of the container at constant pressure,

$Q17$: heat flux exchanged by convection between and the container and the interior 2. It is a function of the temperatures of the interior 2 and the container (T_{int2} , T_t), surface of the container A_r and convective exchange coefficient h_{r-int2} .

$Q18$: reflection heat flux from incident solar radiation by the interior reflectors. It is a function of the reflectivity of the inner reflectors ρ , the surface of the internal reflectors (S_{ref} , n), the transmissivity of glass (τ_g), the solar radiation (G), the angle of the outer reflector (α), the angle and the number of internal reflectors ($\theta_{ref,n}$, 4).

$Q19$: heat flux exchanged by radiation between the container and the fluid. It is a function of the temperatures of the container and the water (T_r , T_f), surface of the container (A_r), emissivity of the container ϵ_r and Boltzmann constant (σ).

$Q20$: heat flux exchanged by convection between the container and the fluid. It is a function of container temperatures and water (T_r , T_f), fluid surface (A_m) and convective exchange coefficient (h_{r-fl}).

✓ **Node 5 :**

At this node, the heat exchange model on the fluid (water) of temperature T_f is written as a function of the container and water temperatures (T_t , T_f), radiating heat fluxes ($Q22$, $Q23$), convective heat fluxes ($Q21$, $Q24$) [22-25]:

(5)

Where,

$m_f \cdot C_{p_f}$: Mass heat of water at constant pressure,

$Q21$: heat flux exchanged by convection between the inner container lid 3 (between the container lid and the fluid surface). It is a function of the temperatures of the container lid and the water (T_t , T_f), the surface of the container lid (A_t) and the convective exchange coefficient (h_{t-int3}).

$Q22$: heat flux exchanged by radiation between the container lid and the fluid. It is a function of the temperatures of the containers and the water (T_r , T_f), the surface of the container lid (A_t), the emissivity of the container (ϵ_t) and the Boltzmann constant (σ).

$Q23$: heat flux exchanged by radiation between the container and the fluid. It is a function of the temperatures of the containers and the water (T_r , T_f), surface of the container (A_r), emissivity of the container (ϵ_r) and Boltzmann constant (σ).

$Q24$: heat flux exchanged by convection between the container and the fluid. It is a function of the temperatures of the container and the water (T_r , T_f), fluid surface A_m and convective exchange coefficient h_{r-int3} .

✓ **Node 6 :**

At this node, the heat exchange model on the temperature thermal storage material T_{st} is written as a function of the temperatures of the container and the thermal storage material (T_r , T_{st}), and the conductive heat flux (Q_{25}) [27]:

$$m_{st} \cdot C_{p_{st}} \frac{dT_{st}}{dt} = Q_{25} \quad (6)$$

$$= \frac{\lambda_{ab}}{e_{ab}} \cdot S \cdot (T_r - T_{st})$$

Where,

$m_{st} \cdot C_{p_{st}}$: Mass heat of thermal storage material,

Q_{25} : flow of heat exchanged by conduction between the container and the thermal storage material. It is a function of the absorbent thermal conductivity temperatures (λ_{ab}), the absorber surface (S) and the thermal storage material mass (m_{st}).

2.3. Equivalent resistance, Power and thermal efficiency of box type solar cooker

In this section, we determine for our structure (Figure 1) the equivalent thermal resistance (R_{eq}), the thermal power which is the thermal flux ($P_{Thermal} = \Phi_{Thermal}$), and the thermal efficiency, which is the ratio between the thermal power and the solar radiation through the glass ($\eta = \frac{P_{Thermal}}{P_G}$). To do this, we use the basic equations of thermal transfer [21] taking into account the following conditions:

- The energy received by the interior of the cooker compensates for the losses by the walls towards the outside of the cooker,
- Inside the cooker, the temperature reached is constant, the wall of the cooker is formed by Wood, Cork and Inox,
- The window of the cooker is formed by the glass 1, air and the glass 2.

In the case of our structure (Figure 1), we can deduce:

- ✓ Thermal resistance $R_{th-walls}$ associated with the equipment of the wall is the sum of the resistance of the wood ($R_{th-wood}$), cork ($R_{th-cork}$) et Stainless steel ($R_{th-inox}$):

$$R_{th-walls} = R_{th-wood} + R_{th-cork} + R_{th-inox}$$

$$= \frac{1}{S} \left(\frac{e_{wood}}{\lambda_{wood}} + \frac{e_{cork}}{\lambda_{cork}} + \frac{e_{inox}}{\lambda_{inox}} \right) \quad (7)$$

Where,

S : Wall surface, equal to 1.5367 m²,

e_{wood}, λ_{wood} : thickness and thermal conductivity of wood, equal to 20 mm and 0.15W.m⁻¹.k⁻¹,

e_{cork}, λ_{cork} : thickness and thermal conductivity of cork, equal to 45 mm and 0.042W.m⁻¹.k⁻¹,

e_{inox}, λ_{inox} : thickness and thermal conductivity of stainless steel, equal to 10 mm and 16.3W.m⁻¹.k⁻¹.

- ✓ The thermal resistance $R_{th-windows}$ associated with the window is the sum of the resistance of the glasses 1 and 2 (R_{th-g}) and that of the air (R_{th-air}):

$$R_{th-windows} = 2 \cdot R_{th-g} + R_{th-air}$$

$$= \frac{1}{Ag} \left(2 \cdot \frac{e_g}{\lambda_g} + \frac{e_{air}}{\lambda_{air}} \right) \quad (8)$$

Where,

Ag : Window area, equal to 0.2401 m²,

e_g, λ_g : thickness and thermal conductivity of glasses 1 and 2, equal to 3 mm and 1W.m⁻¹.k⁻¹,

e_{air}, λ_{air} : thickness and thermal conductivity, equal to 6 mm and 0.042W.m⁻¹.k⁻¹.

- ✓ The power of solar radiation received ($P_{Thermal}$) is the sum of the flows of the wall ($\Phi_{th-walls}$) is the sum of the flows of the wall ($\Phi_{th-windows}$). It depends on the variation of temperatures inside and outside the cooker ($\Delta T = T_{int} - T_{amb}$), and thermal resistance (R_{eq}) :

$$= \frac{\Delta T}{R_{th-walls}} + \frac{\Delta T}{R_{th-windows}} \quad (9)$$

Taking these equations and coefficients, we can deduce:

- ✓ The expression and the value of the equivalent thermal resistance:

$$R_{eq} = \frac{R_{th-walls} * R_{th-windows}}{R_{th-walls} + R_{th-windows}} = 0.51 \text{ K. W}^{-1} \quad (10)$$

- ✓ When $T_{amb} = 29^{\circ}\text{C}$, the value of the thermal power $P_{Thermal}$ for several temperatures T_{int} :

$$\begin{aligned} P_{Thermal} &= 162.74 \text{ W if } T_{int} = 112^{\circ}\text{C, is } \Delta T = 83^{\circ}\text{C,} \\ P_{Thermal} &= 237.69 \text{ W if } T_{int} = 140^{\circ}, \text{ is } \Delta T = 111^{\circ}\text{C,} \\ P_{Thermal} &= 335.29 \text{ W if } T_{int} = 200^{\circ}, \text{ is } \Delta T = 171^{\circ}\text{C.} \end{aligned}$$

- ✓ For solar radiation 990 W/m^2 , the value of solar cooker efficiency:

$$\begin{aligned} \eta &= 68.46\% \quad \text{if } P_{Thermal} = 162.74 \text{ W,} \\ \eta &= 91.56\% \quad \text{if } P_{Thermal} = 237.69 \text{ W,} \\ \eta &= 141\% \quad \text{if } P_{Thermal} = 335.29 \text{ W.} \end{aligned}$$

3. Results and discussion

3.1. Simulation results

3.1.1. Organigram of the numerical code

The numerical resolution of the models of our designed cooker (Equations 1 to 6) is carried out by the Rung Kuta method of order 4 [28] under the C ++ language. We have adopted this method since it has a remarkable accuracy and calculation stability [28]. As shown in the flowchart in Figure 2, the main calculation steps are:

- Declaration of dimensions, thermal data of the Cooker (see Annex 1) and time (T_{max}) and no calculation (h),
- Return of the parameters:
 - Meteorological values: solar radiation values (G), ambient temperature (T_{amb}),
 - Time interval 10 min during operations.
- Initial conditions: initial temperatures of the solar cooker block ($T_{v1}(0)$, $T_{v2}(0)$, $T_{cr}(0)$, $T_r(0)$, $T_f(0)$, $T_{st}(0)$),
- Calculation :
 - When $t \leq T_{max}$, y increasing time by one step of $h=10\text{min}$, the program optimally calculates temperatures desire solar cooker nodes using Rung-kutta methods. At this point, the calculations are performed:
 - ✓ When the ambient temperature (T_{amb}) and the solar radiation (G) are constant or variable with time.
 - ✓ By integration of the differential equations: once at the starting point (RK1), twice at the middle of the interval (RK2 and Rk3), and once at an estimated end point (RK4).
 - Stopping calculations: when $t = 480 \text{ min}$, the program stops the excursions and displays the results obtained from the temperatures with a fourth-order precision (RK4).

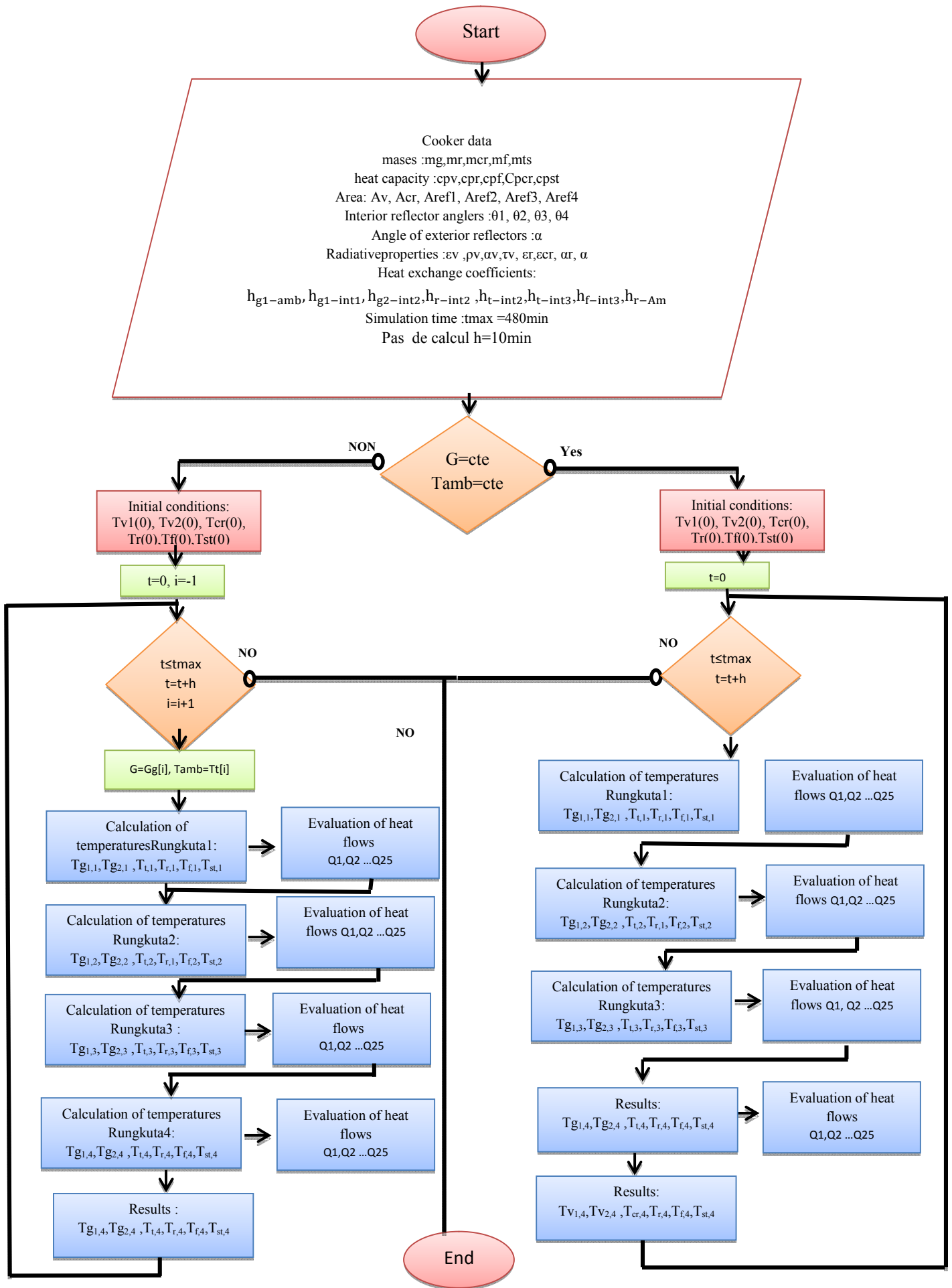


Figure 2: Rung-Kutta method of order 4 flowchart.

3.1.2 Simulation of node temperatures, heat output and cooker efficiency.

3.1.2.1. Transient depending on ambient temperature and solar radiation

In Figure 3, we have shown the typical results of the temperature simulation of the 6 nodes, the power and efficiency thermal of the box type solar cooker for a temperature $T_{amb} = 25^{\circ}\text{C}$ and a solar radiation of 1000 W/m^2 . It clearly appears a behaviour depending on the nodes and the duration of the heating:

- For a node distant from node 1 (Glass 1), the temperature increases gradually over time and becomes saturated after the duration of 3-5 hours. For node 5 (Container: Tf), the maximum temperature (130°C) is reached after 4 to 5 hours,
- As we move away from node 1, the temperature increases and the maximum, of the order 140°C , is obtained for node 3 (lid),
- Between the nodes 1 and 2 (Glass 1 and glass 2), a very important difference of 60°C is obtained. This is due on the one hand to the presence of the vacuum between the glasses and glass 1 close to the external environment (40°C),
- In the node 5 (container) the temperature reached 130°C is slightly lower than that of the lid (Node 3),
- The node 6 corresponding to the storage reaches a significant temperature 110°C close to that of node 2 (Glass 2),
- The thermal power and the efficiency gradually increase and reach the maximum values of 240 W and 170% after 5 hours of heating.

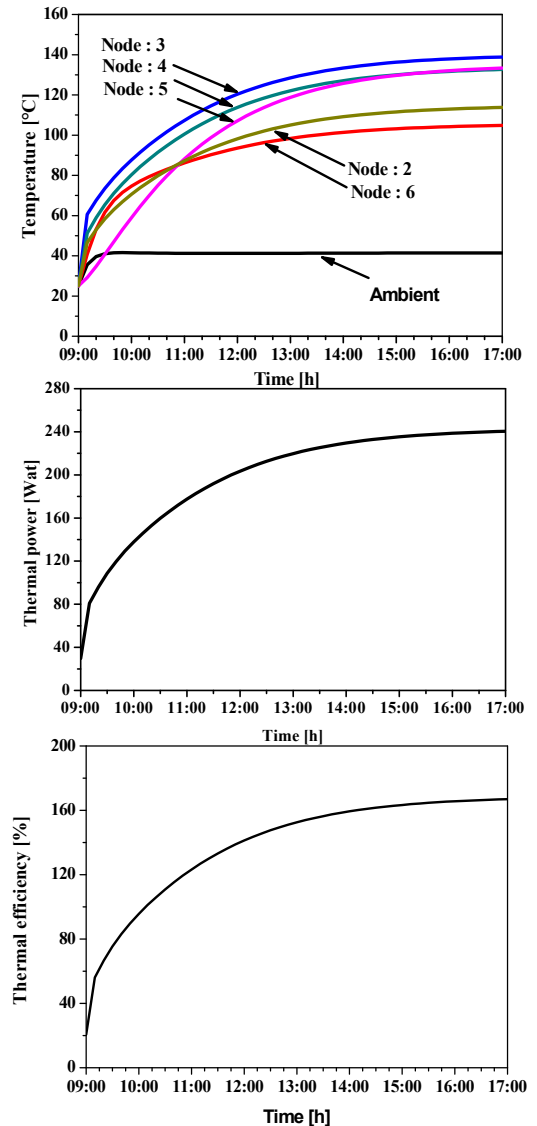


Figure 3: Typical route, during a day, temperatures of 6 nodes, power and efficiency thermal. $T_{amb}=25^{\circ}\text{C}$, solar radiation = 1000 W/m^2 .

Comparing with the recently published results in the literature [22-25,29,30], we deduce comparable behaviors and performances. This shows the good sizing of our cooker and especially the resolution of the differential equations by the Rung-kutta method of order 4.

3.1.2.2. Influence of solar radiation and ambient temperature

In order to analyze the sensitivity of the cooker designed to the variations of the weather conditions, we simulated the influence of the solar radiation the ambient temperature on the temperature of the node, the power and efficiency thermal of the cooker. The obtained results are shown in Figure 4 when the ambient temperature $T_{amb} = 25^{\circ}\text{C}$ and in Figure 5 when the solar radiation is 1000 W/m^2 . The obtained results show that:

- When $T_{amb} = 25^{\circ}\text{C}$, the influence of solar radiation on the temperatures is more marked when one moves away from the neu1 (Glass 1). When the solar radiation increases by 400 W/m^2 , the temperature of the nodes 3 to 6 increases by 60%. These results in increased thermal power and efficiency of 62% and 55%. It should be noted that these variations are also found on other ambient temperatures.
- When the solar radiation = 1000 W/m^2 , the influence of the ambient temperature is not significant. Figure 5 shows that the influence:
 - On the temperatures of nodes 2 to 6 are not marked relative to node 1. When the ambient temperature increases by 40°C , the temperatures of nodes 2 to 6 increase from 7% to 11% and that of node 1 is about 150%.

- When the ambient temperature increases by 40 ° C, the power and efficiency undergo an increase which does not exceed 16% to 20%.

All the results obtained in this section show the strong sensitivity of the cooker to variations in the intensity of solar radiation . As a result, the use of this type of cooker does not depend on the seasons of the year.

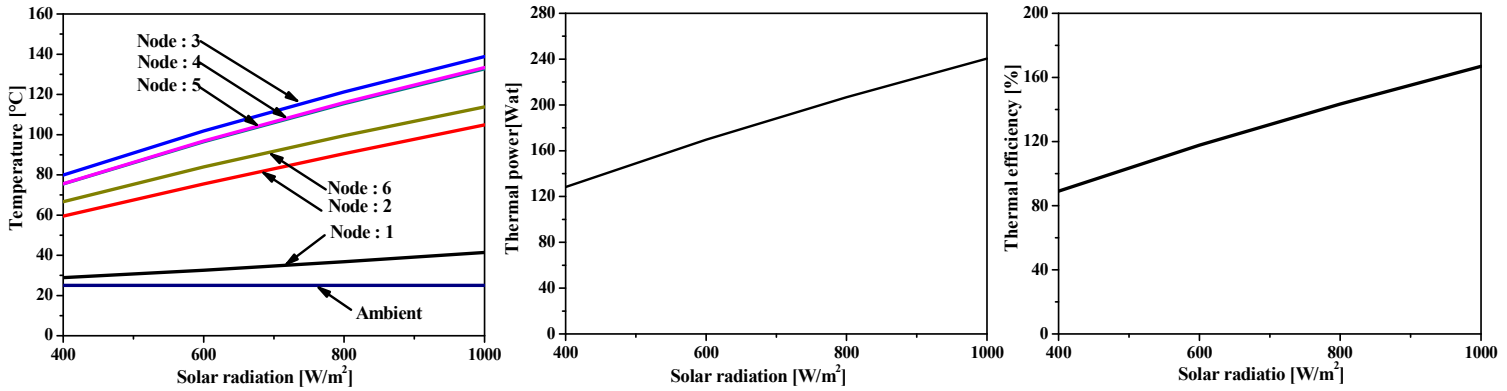


Figure 4: Influence of solar radiation on temperature at each node, thermal power and efficiency. $T_{amb} = 25 \text{ } ^\circ \text{C}$.

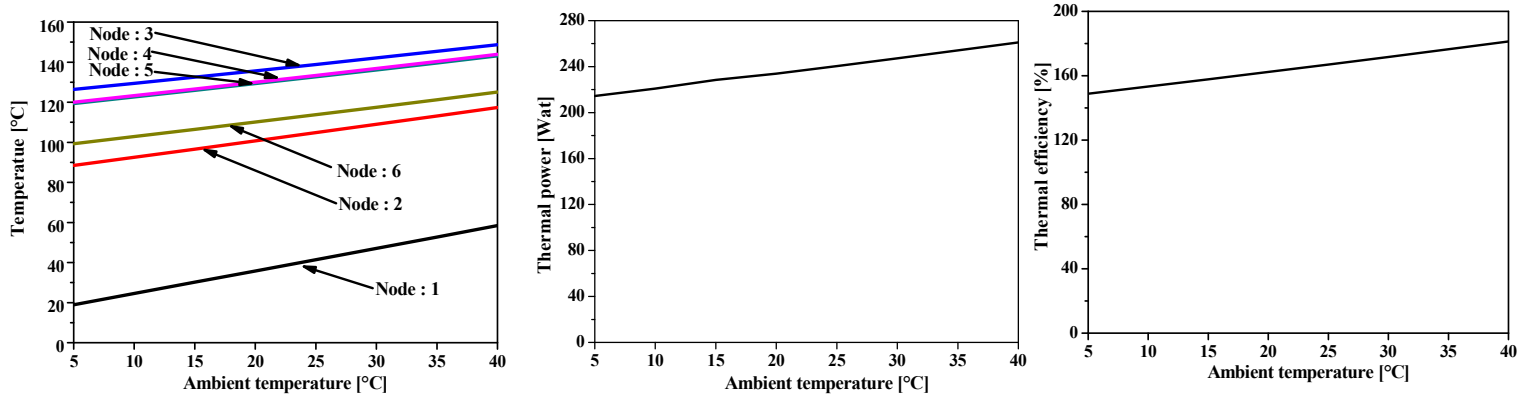
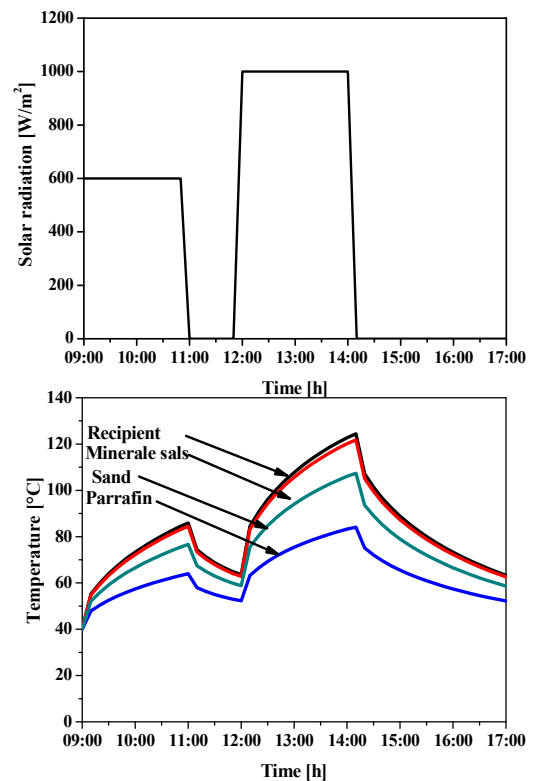


Figure 5: Influence of the ambient temperature on the temperature at each node, the thermal power and efficiency. Solar radiation = 1000 W / m^2 .

3.1.2.3. Thermal storage analysis

In order to analyze the thermal storage in the cooker, we simulated, when the ambient temperature $T_{amb} = 40 \text{ } ^\circ \text{C}$ and the variable solar radiation, the influence of the thermal storage (mineral salt, sand, paraffin) on the temperature of the knot 4 (recipient) and the thermal power of the cooker according to the solar radiation (figure 6). In equations 1 to 6, we did not take into account the mutual influence of thermal exchanges between the nodes. These behaviors will be published in other works. The simulation results show:

- The temperature profile of the mineral salt is very close to that of the container.
- During heating under the solar radiation of 600 W / m^2 and 1000 W / m^2 , the maximum temperatures of mineral salt (node 6) and recipient (node 4) reach $84 \text{ } ^\circ \text{C}$ and $120 \text{ } ^\circ \text{C}$, the maximum thermal power 146 Watt and 101%,
- In the absence of solar radiation, the relaxation of the thermal magnitudes of the mineral salts and the container are similar



and depend on the intensity of the solar radiation. After one hour of relaxation, we can deduce decreases in temperature of 25% and thermal power of 19 to 25%.

All the results obtained show that the thermal behaviour of salt is very beneficial in a cooker to store the temperature and use it during sudden changes in the intensity of solar radiation. Decreases in temperature by 25% after one hour are largely sufficient to ensure or finish cooking by the cooker users.

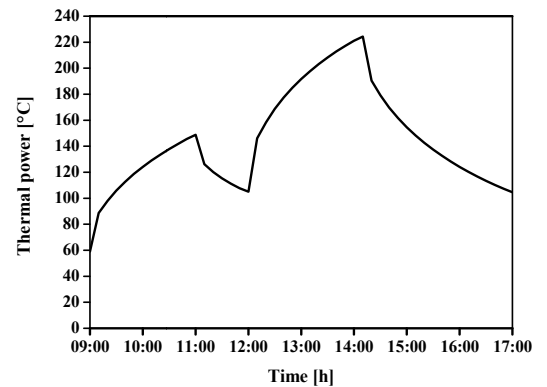


Figure 6: Influence of solar radiation on thermal temperatures and powers of the thermal storage (Node 6) and the recipient (Node 4) of the solar cooker. $T_{amb} = 40\text{ }^{\circ}\text{C}$.

3.2. Experimental results and validation

2.1. Dimensioning of the box type solar cooker

We sized the solar cooker respecting the needs of the beneficiaries to heat a volume of $50\text{ cm} * 50\text{ cm} * 30.5\text{ cm}$ (0.07625 m^3) with 4 reflectors. The different stages of realisation of this cooker are:

- Dimensioning of the absorber (Figure 7A), consisting of a black painted stainless steel plate of size: $L = 50\text{ cm}$, $l = 50\text{ cm}$, thickness = 1 mm.
- Dimensioning of the thermal storage material (Figure 7B) of dimensions: $L = 50\text{ cm}$, $l = 50\text{ cm}$, thickness = 0.5 cm).
- Dimensioning of the double glazing (Figure 7C), formed by two panes, spaced 0.6 cm, dimension: $L = 49\text{ cm}$, $l = 49\text{ cm}$. This transparent cover is used for creating the greenhouse effect and insulation to limit heat loss.
- Dimensioning of the inner box (Figure 7D), formed by stainless steel of dimensions: $L=50\text{cm}$, $l=50\text{ cm}$, $H=34\text{cm}$. The choice of this material is justified by its very good reflection coefficient of the order of 90% and a lifetime of 15 years.
- Dimensioning of the outer box (Figure 7E), consisting of the outside of the wood (of dimensions: $L = 62\text{ cm}$, $l = 62\text{ cm}$, $h = 40\text{ cm}$) and the cork (of dimensions: $L=60\text{ cm}$, $l=60\text{cm}$, $h=40\text{ cm}$) from the inside. This box strengthens the insulation of the walls, particularly by the Cork which is considered a very good thermal insulation conductivity 0.0042 W/m.k , natural nontoxic and efficient.
- Dimensioning of the mirror reflector (Figure 7F): length $L = 80\text{ cm}$, width $l = 60\text{ cm}$.
- Sizing of the solar cooker door (Figure 7G), formed by the wood with the sealing of rectangular asbestos ($L = 33\text{ mm}$, $l = 26\text{ mm}$).
- Prototype defines (Figure 7H) to experiment in the laboratory.

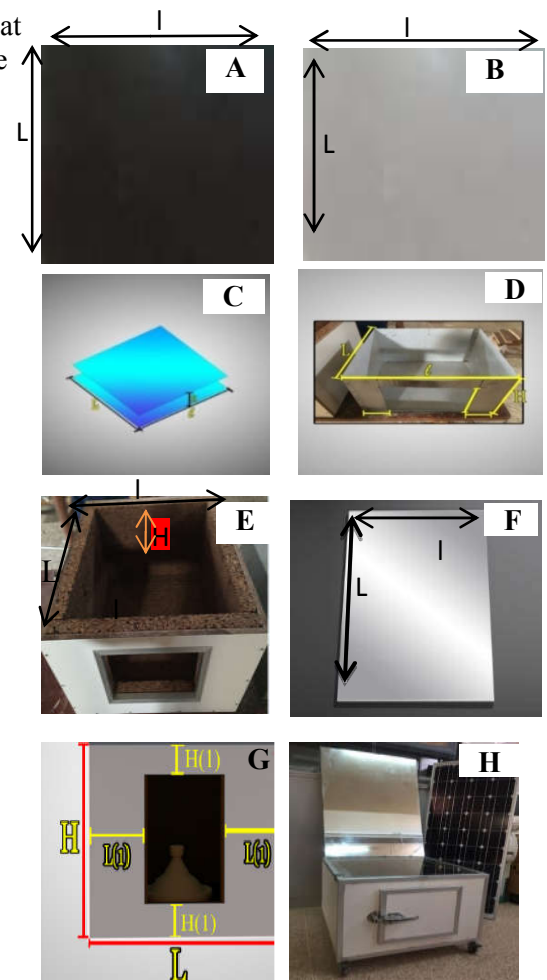


Figure 7: Dimensioning of the solar cooker prototype.

3.2.2. Experimental procedure

The prototype designed (Figure 7H), studied in Section 3.1, is tested using the fully automated test bench in the laboratory (Figure 8). As shown in FIG. 8, this bench is formed by:

- Box type solar cooker ,
- CMP6 pyranometer and temperature sensors to measure the intensity of solar radiation and ambient temperature. This equipment is connected to the Digital Multimeter (Keithley Model 2700).
- Digital millimeters (Keithley Model 2700), connected to the CM6 Pyranometer, temperature sensors and PC. Its role is to perform voltage measurements, on 40 different channels, and via the GPIB and RS232 interface, the PC deduces and displays the intensity of the solar radiation, the ambient temperature and the different temperatures of the nodes.

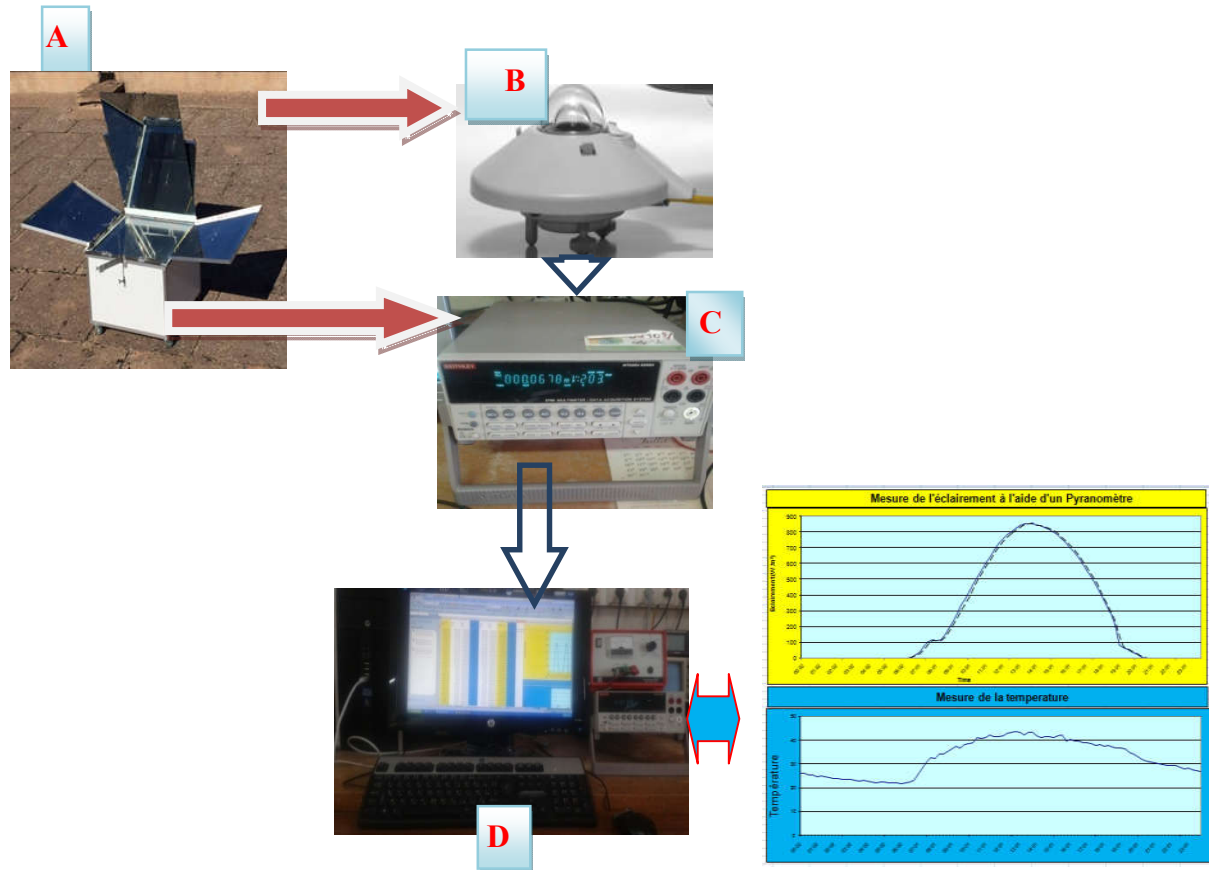


Figure 8 : Measurement benches set up in the laboratory.

- A :** Box type solar cooker with additional reflectors,
- B :** CMP6 pyranometer and temperature sensors,
- C :** Digital Multimeter (Keithley model 270, 40 channels),
- D:** PC acquisition and display.

3.2.3. Experimental results

3.2.3.1. Typical operation all day

We have characterised, for a whole day, the operation of the solar cooker of Figure 7H with a reflector (mirror) and a container inside the cooker. We noted the intensity of the solar radiation, the external and container temperatures (Node4), the thermal power and efficiency of the cooker. The typical results obtained are shown in Figure 9. In the same figures, concerning the temperature of the node 4, the power and the efficiency, we have represented the simulation results, taking into account the meteorological conditions (Solar radiation and external temperature) and cooker settings (Appendix 1). The results obtained show that:

- The solar radiation reaches 1019.76 W/m^2 and the ambient temperature $35 \text{ }^\circ\text{C}$ around 12h40 min,
- Good agreement between experimental results and simulated results,
- When the solar radiation varies from 400 W/m^2 , the temperature of the container varies from $55 \text{ }^\circ\text{C}$ to $88 \text{ }^\circ\text{C}$ (an increase of 60%), the thermal power and efficiency vary respectively from 85 W to 135 W (or an increase of 59%) and 43% to 65% (an increase of 51%).
- The optimal operation of the cooker is obtained at 12h40min. The container temperature, the power and the thermal efficiency respectively reach $110 \text{ }^\circ\text{C}$, 168 Watt and 75%.

Comparing these results with those of simulations (paragraph 3.1.2.2.), we deduce a very good agreement in terms of the influence of the intensity of solar radiation on the operation of the cooker. Moreover, the comparison with the results of literature [22-25, 37, 38], we can deduce very interesting performances on our box type cooker.

All the obtained results show, on the one hand, the feasibility of the solar cooker sized and produced during this work, and, on the other hand, the validation of the calculation code adopted for this type of box type solar cooker.

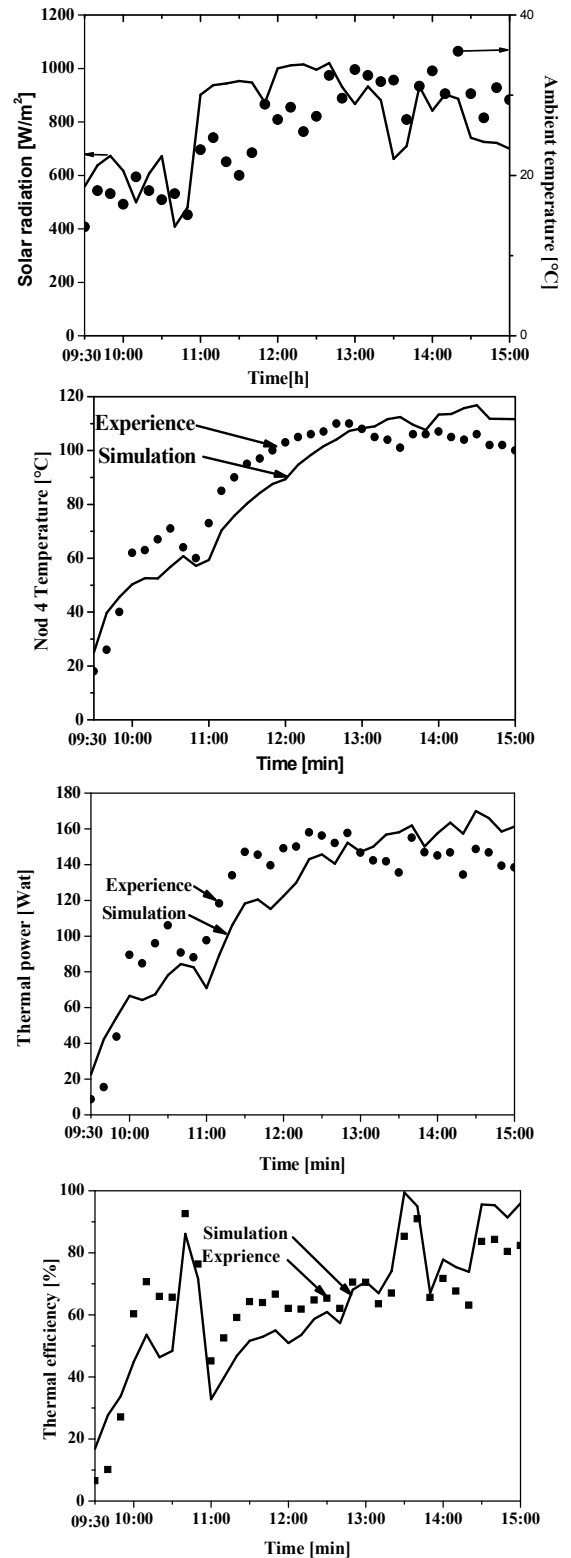


Figure 9: Experimental plot of the meteorological conditions (solar radiation and external temperature), experimental and simulated temperature of the recipient (Node 4), the thermal power and efficiency of the box type solar cooker with a reflector (mirror).

3.2.3.2. Relaxation of the container temperature (node 4).

In order to estimate the relaxation of node 4 (recipient), we experienced the cooker, without the thermal storage, according to the sequences:

- Heating for 3 hours,
- Then stop the capture of the solar radiation by the reflector.

During this experiment, we noted, as previously, the solar radiation, the ambient temperature, the temperature of the container, the thermal power and efficiency of the cooker. The results obtained as well as those of the numerical simulations are shown in Figure. 10. In the absence of solar radiation, the efficiency of the cooker is not represented since the solar radiation is zero. The set of results shows:

- For each sequence, we observe a very good agreement between experience and simulation,
- When the solar radiation is at the maximum intensity (1000 W/m^2), the recipient temperature, thermal power and efficiency reach their maximum values: 112°C , 161 Watt and 67% .
- In the absence of solar radiation :
 - ✓ the external temperature is stable (30°C),
 - ✓ The temperature of the container undergoes a relaxation of the duration of $1\text{h}45\text{mn}$. It varies from 112°C to 59°C (a decrease of 50%). This results in a decrease of the thermal power from 161 W to 61 W .
 - ✓ During a 1 h of relaxation, the temperature decreases from 104°C to 75°C (diminution of 24%) Thermal power varies from 150 W to 100 W (diminution of 33%).

Comparing these results with those simulated (paragraph 3.1.2.3), we deduce a very good agreement in terms of thermal relaxation. The comparison with the results of the literature [39], we can conclude very interesting performances on our cooker. All of the results obtained in this section show, on the one hand, the good thermal insulation of the cooker is designed and realised and, on the other hand, the validation of the numerical code is developed during this work.

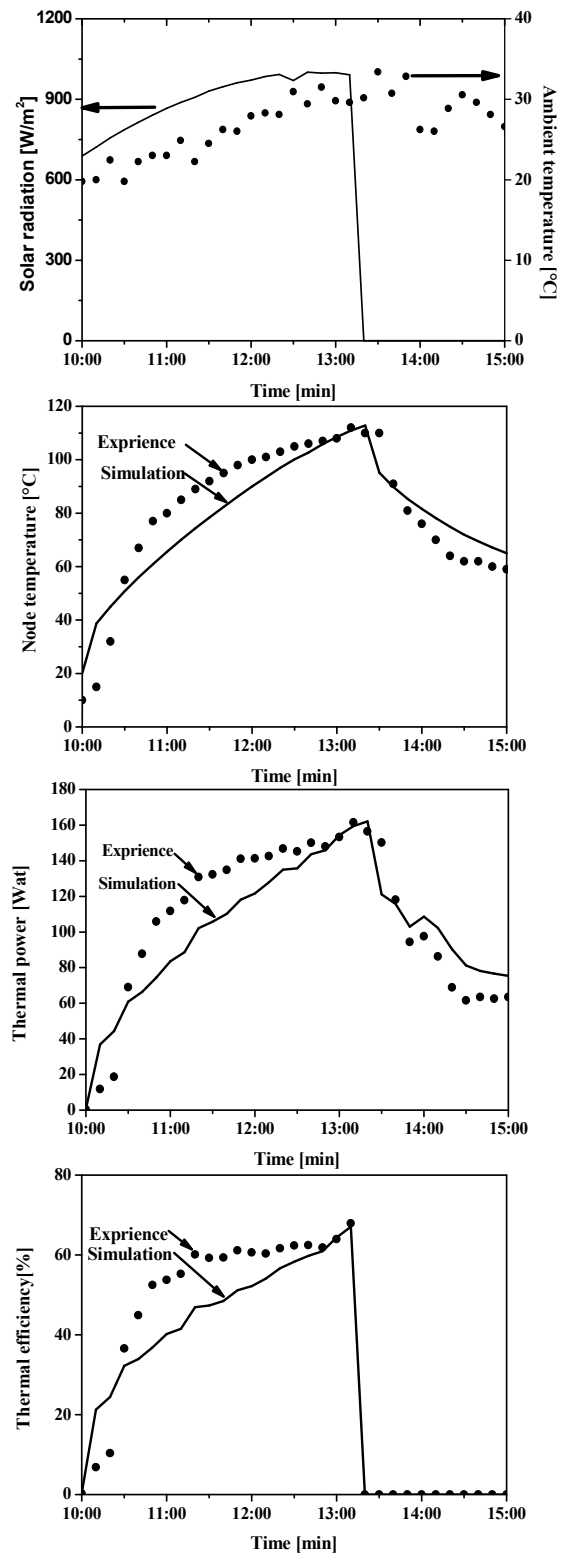


Figure 10: Experimental plot of the meteorological conditions (solar radiation and external temperature), experimental and simulated temperature of the recipient (Node 4), the power and thermal efficiency of the solar cooker box with a reflector (mirror).

3.2.2.3. Temperature storage

We have experimented the efficiency of the storage of the temperature by heating then stopping the solar radiation in the presence of the storage by the mineral salt. The typical results (solar radiation, ambient temperature, temperature of the container and the salt, thermal power and efficiency) obtained are shown in Figure. 11. In the same figures which represent the temperatures of the container and salt, power and efficiency, we have plotted the results of the numerical simulations taking into account the conditions of the experiment and the parameters of the cooker (Annex 1). These results show:

- Mineral salt temperature profiles are very close to container profiles. This behaviour confirms the simulation results (Figure 11).
- A very good agreement between the experimental results and the simulated ones,
- During heating, the maximum temperatures of mineral salt (node 6) and container (node 4) reach respectively 137°C and 146 °C, maximum power and efficiency respectively 216 Watt and 104%,
- In the absence of solar radiation, the temperature of the container and the thermal power undergo a relaxation, lasting 2h30mn. They vary respectively from 146 ° C to 74 ° C (a decrease of 50%) and 216 W to 118 W (a decrease of 45%).
- At the end of a one-hour of relaxation, we can deduce a decrease in temperature from 160 ° C to 95 ° C (40%) and from 243 W to 150 W (38%). Comparing with the previous results, without the presence of thermal storage, we can conclude, for this experiment. The effect of storage is not significant.

The first results on storage, obtained in this section, show the validation of the results of the simulations in terms of the behaviour of the nodes 4 and 6 (same behaviour). However, the role of storage in the cooker is not significant. This is due to the positioning of the storage at the bottom of the cooker. We think that the positioning of the room also plays a key role in improving the performance of the cooker. To do this, work is in progress.

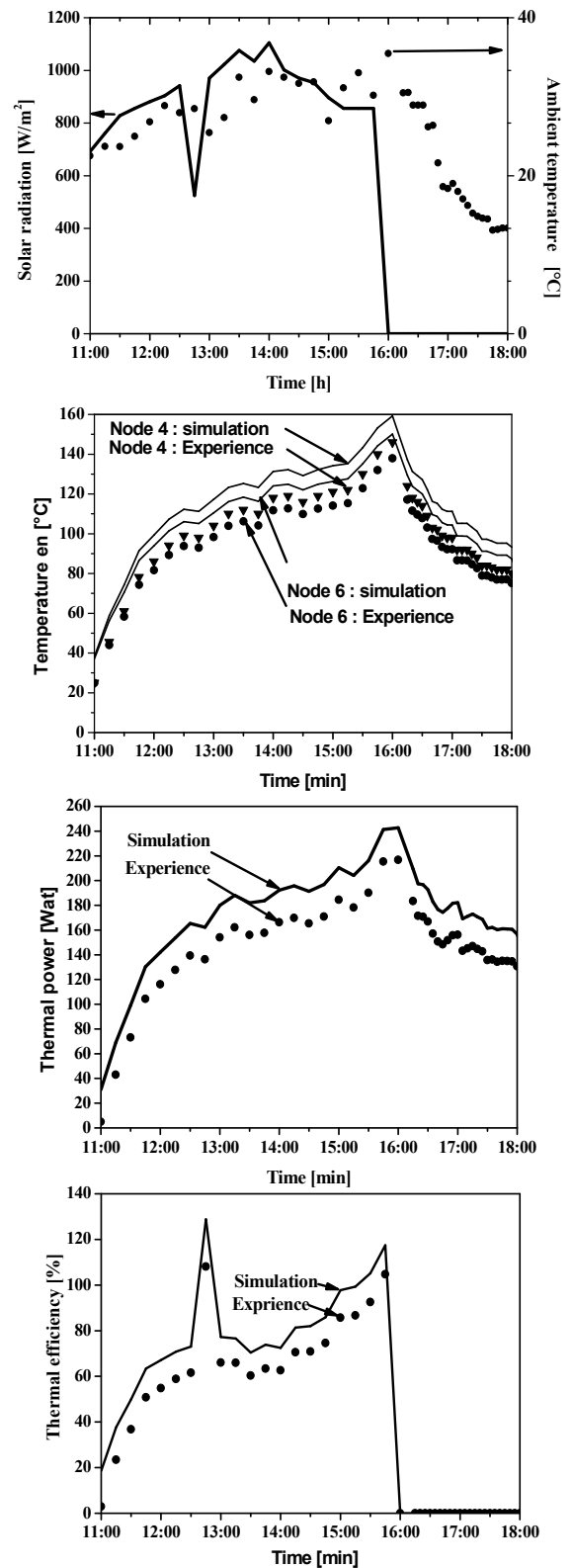


Figure 11: Experimental plot of the meteorological conditions (solar radiation and external temperature), experimental and simulated temperature of Nodes 4 and 6, the thermal power and efficiency of the box type solar cooker with a reflector (mirror).

Conclusion

In this article, we designed and realize a four-reflector box type solar cooker with thermal storage. The sizing and the study of the cooker is based on the development of a numerical code of the equations of the heat transfer equilibrium of transient heat transfer. The results obtained show:

- Good agreement between simulation and experience,
- Very satisfactory energy performance: thermal resistance 0.51 K.W^{-1} , temperature, thermal power and efficiency respectively exceeding $120 \text{ }^\circ\text{C}$, 160 Watt and 70%,
- The influence of the intensity of the solar radiation is more than that of the ambient temperature. As solar radiation increases by 400 W/m^2 , the temperature, power and thermal efficiency increase by 60%, 62% and 55% respectively. On the other hand, when the temperature increases by $40 \text{ }^\circ\text{C}$, the temperature, the power and the thermal efficiency increase respectively by 16 to 20%.
- The presence of storage only at the bottom of the cooker did not show any significant improvement.

All the obtained results show the validation of the numerical code developed during this work and, consequently, the feasibility of the prototype conceived and realised in the laboratory. This represents an interesting contribution in the field of solar cookers without storage. To improve the energy performance of the cooker, work is underway on thermal storage to stabilize, especially, the temperatures inside the cooker, following sudden changes in solar radiation.

Nomenclature

A: Area (m^2)

h: Heattransfer convection coefficient ($\text{W/m}^2\text{k}$)

T: Temperature ($^\circ\text{C}$)

T_{int} : Temperature inside the furnace

t: Time (s)

G: Incidental solar radiation (w/m^2)

Cp_w : Specific heat of water

$R_{th-walls}$: Thermal resistance of the walls (k.w^{-1})

e_{wood} : Thermal resistance of wood (m)

λ_{wood} : Thermal conductivity of wood (W/m.k)

e_{liege} : Thickness of cork. (m)

λ_{liege} : Cork thermal conductivity of crok (W/m.k)

e_{inox} : Thickness of stainless (m)

λ_{inox} : Thermal conductivity of stainless steel. (W/m.k)

$R_{th-Windows}$: Thermal resistance of glass (k.w^{-1})

R_{th-g} : Thermal resistance of glass. (k.w^{-1})

R_{th-air} : Thermal resistance of air. (k.w^{-1})

e_g : Thickness of glass

λ_g : Thermal conductivity of glass. (W/m.k)

e_{air} : Thickness of air (m)

λ_{air} : Thermal conductivity of air (W/m.k)

Φ_T : Fluxthermique total (W)

$\Phi_{th-Walls}$: Heat flow of the walls. (W)

$\Phi_{th-Windows}$: Thermal flow of windows. (W)

Subndex

g: Glass

amb: Ambient

al: Aluminum

e: Thickness

ex: External

st: Storage

ab: Absorber

r: Cooking pot

w: Water

c: Sky

t : lid of the recipient

int1 : Inner (between glazing 1 and glass 2)

int2 : Inner 2 (between glass 2 and the indoor environment)

int3 : Inner 3 (between the container lid and the fluid surface)

Greekletters

σ : Stefan-Boltzman constant ($5.669 \cdot 10^{-6} \text{ w/m}^2\text{K}^4$)

ρ : Reflectivity

ε : Emittance

α : Absorptance

τ : Transmittivity

λ : Thermal conductivity

References

- 1.S. Bilgen, *Ren. Sust. Energy Rev.* 38 (2014) 890-902.
- 2.R. S.Dhillon, and George von Wuehlisch. *J. Biom. bioe.* 48 (2013) 75-89.
- 3.M. L. Madignier, G.Benoit, & Roy, C. *CGAAER, rapport*, 14056 (2014) 56.
- 4.N.Panwar,S.Kaushik, S.Kothari, *Ren. Sust. Energy Rev.* 16(6) (2012) 3776.
- 5.K.Schwarzer, M.E.V.da Silva,*Solar energy* 82(2) (2008) 157.
- 6.B.H.K.Ibrahim, V.Jose, *Inter. J. Engin. Sci. Res. Tech.* 5(7) (2016) 169.
- 7.S.Kumar, *Ren. Energy*, 30 (2005) 1117-1126.
- 8.E. H. Amer, *Energy Conv. Manag.*44(16) (2003) 2651-2663.
- 9.S. Z. Farooqui, *Solar Energy* 92 (2013) 62-68.
- 10.A. A. El-Sebaili,A. Ibrahim, *Renewable energy*, 30(12) (2005)1861-1871.
- 11.N. M.Nahar, *J. engine. sci. tech.*, 4(3) (2009) 264-271.
- 12.A.Harmim, M.Belhamel, M.Boukar, M.Amar, *Energy* 35 (2010) 3799-3802.
- 13.H.Terres, S.Chávez, A.Lizardi, R.López, M.Vaca,J. Flores, A.Salazar,*In Journal of Physics: Conference Series* 582(1) (2015) 12024.
- 14.B. Z.Adewole, O. T.Popoola, A. A.Asere, *Inter. J. Energy Engin.* 5(5) (2015) 95.
- 15.M.Abu-Khader, M.Abu Hilal, S.Abdallah,O.Badran, *Jor. J. Mech. Ind. Engin.*5(1) (2011).
- 16.E. O.Akoy, A. I.Ahmed, *J. Agr. Sci. Engin.* 1(2) (2015) 75.
- 17.S. B.Joshi, A. R.Jani, *Solar Energy* 122 (2015) 148.
- 18.S. B.Joshi, A. R. Jani, *Proceedings of the 5th Nirma University International Conference on Engineering, Ahmedabad, India, November 26-28 2016.*
- 19.S. B.Joshi, A. R.Jani, *Ren. Energy*, (2013) 2013.
- 20.S. B.Joshi, A. R. Jani, Certain analysis of a solar cooker with dual axis sun tracker. In *Engineering (NUIcONE), 2013 Nirma University International Conference on IEEE* (2013, November) pp. 1-5.
- 21.A.DEGIOVANNI,*Tech. Ing.* (1999)
- 22.H.Terres, S.Chavez, R.Lopez, A.Lizardi,A. Lara, J. R.Morales, *In Proceedings of the ASME 2015 9th International Conference on Energy Sustainability* (2015).
- 23.H.Terres-Peña, J.Morales-Gómez, A.Lizardi-Ramos, R.López-Callejas,R.d.J. Portillo-Vélez, *Rev. Int. métodos numér. Cál. Diseño Ing.* 29(2) (2013) 122.
- 24.H. Terres-peña, A.Lizardi-ramos, R.López-callejas, M.Vacamier, *Rev. Proto. Tecn.* 10 (2016).
- 25.H.Terres, A.Lizardi, R.López, M.Vaca, S.Chávez, *Energy Procedia* 57 (2014) 1583.
26. W.Swinbank, CQJR. *Quart. J. Royal Meteorol. Soc.* 89.381 (1963): 339-348.
- 27.S. Talbi, K.Kassmi, R.Malek, *In Renewable and Sustainable Energy Conference (IRSEC), 2016 International* (2016, November) (pp. 348-352). IEEE.
- 28.U. M.Ascher, L. R. Petzold,*Computer methods for ordinary differential equations and differential-algebraic equations* 61(1998)
- 29.E. Cuce, P. M. Cuce, *Inter. J. Low-Carbon Techn.* 10(3) (2013) 238-245.
- 30.C.Ali, K.Rabhi, S.Attyaoui, I.Jallouli, H. B. Bacha, *Inter. J. Res. Rev Applied Sci.* 3(3) (2010).
- 31.V. P.Sethi, D. S.Pal, K. Sumathy, *Energy Conver. Manag.* 81 (2014) 231-241.
- 32.D.Buddhi, S. D. Sharma, A. Sharma, *Energy Conver. Manag.* 44(6) (2003) 809-817.
- 33.D. Tarwidi, *In Information and Communication Technology (ICoICT), 2015 3rd International Conference* (2015, May) (pp. 584-589). IEEE.
- 34.N. M. Nahar, *Energy Conver. Manag.* 44(8) (2003) 1323-1331.
- 35.M. R. I. Ramadan, S. Aboul-Enein, A. A. El-Sebaili, *Solar wind. techn.* 5(4) (1988) 387-393.
- 36.D.Buddhi, L. K. Sahoo, *Energy Conver. Manag.* 38(5) (1997) 493-498.
- 37.H.Kurt, E. Deniz, Z. Recebli, *Inter. J. Green Energy*, 5(6) (2008) 508-519.
- 38.V. P. Sethi, D. S.Pal, K. Sumathy, *Energy Convers. Manag.* 81 (2014) 231-241.
- 39.A. Soria-Verdugo, *Energy Sust. Develop.* 29 (2015) 65-71.

Annex1

Masse (Kg)

- Masses of glass ($m_g = m_{g1} = m_{g2}$) : 6.5,
- Container lid mass (m_r) : 0.2,
- Paraffin mass (m_p) : 7.5,
- Mass of sand (m_s) : 7.5,
- Mass of mineral salts (m_{pNaCl}) : 7.5kg,

Heat capacity (J/kg-k)

- Heat capacity of glass ($C_{pg1} = C_{pg2} = C_{pg}$) : 800,
- Heat capacity of container lid (C_{pt}) : 900,
- Heat capacity of paraffin (C_p) : 2165,
- Heat capacity of sand (C_{ps}) : 1000 ,
- Heat capacity of mineral salt (C_{pNaCl}) : 920,

Area (m^2)

- Area of glass ($A_{g1} = A_{g2} = A_g$) : 0.2401,
- Area of container lid (C_{pt}) : 0.0201,
- Area of recipients (A_t) : 0.0804,
- Area of interior reflector: $S_{ref,1} = S_{ref,2} = S_{ref,3} = S_{ref,4} = 0.015625$,

Angle (Degree)

- Angle de réflecteur intérieure : $ref, 1 = ref, 2 = ref, 3 = ref, 4 = 0.015625$,
- Additional reflector angle (mirror) to the horizontal glass surface $\alpha = 120$,

Coefficient of heat exchange by convection ($W/m^2.k$) [25]

- Between glass 1 and glass 2 (h_{g1-amb}): 13.3
- Between glass 1 and inner 1 ($h_{g1-int1}$): 3.8
- between glass 2 and inner 2 ($h_{g2-int2}$): 4.4
- Between the lid of recipient and the inside 2 (h_{t-int2}): 4.4
- Between the recipient and the interior 2 (h_{r-int2}): 4.4
- Between the lid of recipient and the inner 3 (h_{t-int3}): 4.4
- Between the fluid and the interior 3 (h_{f-int3}): 4
- Between the recipient and the fluid 3 (h_{r-am}) : 4

Radiative properties (Dimension less)[25]

- of glass (α_g) : 0.17, (τ_g) : 0.48, (ϵ_g) : 0.35
- of container lid (α_t) : 0.9, (ϵ_t) : 0.85
- of recipient (ϵ_r) : 0.89
- of mirror (ρ) : 0.9

Constante de Boltzmann : $5.669 \cdot 10^{-6} \text{ w/m}^2\text{K}^4$.

(2018); <http://www.jmaterenvirosnci.com>